

Can brane cosmology with a vanishing Λ explain the observations?

R. G. Vishwakarma* and Parampreet Singh†
*Inter-University Centre for Astronomy and Astrophysics,
 Post Bag 4, Ganeshkhind, Pune-411 007, INDIA.*

A plethora of models of the universe have been proposed in recent years claiming that the present universe is accelerating, being driven by some hypothetical source with negative pressure collectively known as *dark energy* which though do not appear to resemble any known form of matter tested in the laboratory. These models are motivated by the high redshift supernovae Ia observations. Though low density models, without dark energy, also appear to fit the SN Ia data reasonably well, however, they are ruled out by the CMB observations.

In this paper, we present a warped brane model with an additional surface term of brane curvature scalar in the action. This results in shifting the *dynamical curvature* of the model from its *geometrical* counterpart, which creates profound consequences. Even for $\Lambda = 0$, the low energy decelerating model successfully explains the observed locations of the peaks in the angular power spectrum of CMB. The model also fits the high redshift supernovae Ia observations, taken together with the recently observed SN 1997ff at $z \approx 1.7$. Additionally, it also fits the data on the angular size and redshift of the compact radio sources very well.

PACS numbers: 9880, 9880E, 9880H, 0420

I. INTRODUCTION

In the past few years, there has been a spurt of activity in discovering models of the universe in which the expansion is accelerating, fuelled by some self-interacting smooth unclustered fluid with high negative pressure collectively known as *dark energy* (for a recent review, see [1]). These models are mainly motivated by the high redshift SuperNovae (SN) Ia observations which cannot be explained in the framework of the canonical Einstein deSitter model (a model of the decelerating expansion of the universe). The *dark energy*-models are also supported by the recent measurements of the fluctuations in the power spectrum of the cosmic microwave background (CMB) radiation which appear to indicate that the universe is spatially flat and, hence, $\Omega_{\text{total}} \approx 1$ [2, 3]. However, the contribution from the total mass density, including the dark matter, is only about one third: $\Omega_{\text{m}0} \approx 0.3$, which comes from the studies of the evolution of cluster abundances with redshift, measurements of the power spectrum of large-scale structure, analyses of measured peculiar velocities as they relate to the observed matter distribution, and observations of the outflow of material from voids [4] (the subscript 0 denotes the value of the quantity at the present epoch). Thus, the remaining two thirds of Ω_{total} can easily be accounted by the *dark energy*.

The simplest model for *dark energy* is the cosmological constant Λ , which is though plagued with the so called the cosmological constant problem: why don't we see the large vacuum energy density $\rho_v \equiv \Lambda/8\pi G \approx 10^{76}$ GeV⁴, expected from particle physics which is $\approx 10^{123}$ times larger than the value predicted by the Friedmann equation? A phenomenological solution to this problem is supplied by a dynamically decaying Λ [5, 6, 7] or by an evolving large-scale scalar field, commonly known as *quintessence*, which can produce negative pressure for a potential energy-dominated field [1]. A plethora of models of *dark energy* has erupted from these ideas in the past few years claiming that the present universe is accelerating [1]. It should be noted however that despite its consistency with the observations, the nature of *dark energy* is a mystery at present. It does not seem to resemble any known form of matter tested in the laboratory. As yet, we have no direct indication that it really exists. In fact, a more natural value of the cosmological constant is zero (which could either be due to some symmetry or due to a dynamical adjustment mechanism) rather than an extremely small value but still non-zero. There have been numerous suggestions that the apparent complications can be eliminated by modifying the laws of gravity [8].

In this paper, we show that the present observations – measurements of the angular fluctuations in the power spectrum of the CMB, magnitude-redshift observations of the high redshift SN Ia including SN 1997ff of $z \approx 1.7$, angular size-redshift observations of the radio sources of size milliarcsecond – can successfully be explained *without* a Λ -term and the universe is still decelerating. The background model, we consider for this purpose, comes from the warped brane cosmology with an addition of a brane curvature scalar in the action. Higher dimensional (brane) models, inspired by the superstring theory solutions, are acquiring attention. One possibility of great importance

* e-mail: vishwa@iucaa.ernet.in

† e-mail: param@iucaa.ernet.in

arising from these models is that the fundamental Planck scale in the higher dimensions can be considerably smaller than the usual Planck scale in our 4-dimensional spacetime. This would have profound consequences for models of the very early universe. For ready reference and also for completeness, we describe the model in the next section. Observational and cosmological consequences of the model are studied in the following sections.

II. THE MODEL

In brane cosmology, the homogeneous, isotropic Robertson Walker (RW) universe can be envisioned as a hyper surface embedded in the Schwarzschild anti-deSitter (AdS) bulk spacetime. For the RW metric

$$ds^2 = -dt^2 + S^2(t) \left(\frac{dr^2}{1 - kr^2} + r^2 d\theta^2 + r^2 \sin^2 \theta d\phi^2 \right), \quad (1)$$

the Israel junction conditions [9] yield a Friedmann-like equation which has some additional terms [10, 11, 12]:

$$H^2 = \frac{8\pi G}{3} \rho \left(1 + \frac{\rho}{2\sigma} \right) + \frac{\lambda}{3} + \frac{C}{S^4} - \frac{k}{S^2}, \quad (2)$$

where S is the scale factor, G and λ are respectively 4-D gravitational and cosmological constants, σ is the brane tension and C is the mass parameter of the bulk black hole. The energy density $\rho = \rho_m + \rho_r$ ($\rho_m \equiv \rho_{\text{matter}}$, $\rho_r \equiv \rho_{\text{radiation}}$), where ρ_m has contributions from baryonic as well as dark matter (discrepancies between the apparent baryon content of galaxies and galaxy clusters and their dynamically inferred masses). Equation (2) differs from the usual Friedmann equation of the standard cosmology in the following two terms. Firstly, the ρ^2 term which arises from the corrections in the stress tensor, by imposing the junction conditions; and secondly, the *dark radiation* term C/S^4 , which arises from the projection of Weyl curvature of the bulk black hole on the brane and behaves like an additional collisionless and isotropic massless component. However, as we shall show later, these modifications die out at low redshifts.

If one considers quantum corrections to the bulk-brane action, then further modifications to the Friedmann equation can be obtained. One such correction, which is also needed for stress tensor regularization [13], has been widely discussed in the brane world scenarios [14, 15, 16]. It is achieved by adding the Ricci curvature scalar of the brane as a surface term in the action. In warped brane models, this shifts the curvature parameter k ($= 0, \pm 1$) of the RW metric to $k_{\text{eff}} \equiv k - \alpha$ and equation (2) leads to [14, 16]

$$H^2 = \frac{8\pi G}{3} \rho \left(1 + \frac{\rho}{2\sigma} \right) + \frac{\Lambda}{3} + \frac{C}{S^4} - \frac{(k - \alpha)}{S^2} \quad (3)$$

where

$$\alpha = b \left[\sqrt{\frac{\pi G \sigma}{3}} l - \frac{1}{16 \pi G \sigma l^2} \right], \quad (4)$$

$$\Lambda = \lambda - \frac{3b}{l} \sqrt{3\pi G \sigma} \left[\frac{8\pi G \sigma l^2}{9} + \frac{1}{4\pi G \sigma l^2} - 1 \right], \quad (5)$$

$$C = C \left[1 + b \left(\frac{3 - \beta^2}{3\beta} \right) \right], \quad \beta = 4l \sqrt{\frac{\pi G \sigma}{3}}. \quad (6)$$

Here b is a small dimensionless parameter through which the brane curvature couples to the action and l is the radius of curvature of the bulk spacetime. Equation (3) provides the model which we shall be considering in this paper. Some cosmological implications of this model have been studied earlier by considering a non-zero Λ [16].

By interpreting the different energy density components in units of the critical density, in the usual forms:

$$\Omega_m \equiv \frac{8\pi G}{3H^2} \rho_m, \quad \Omega_r \equiv \frac{8\pi G}{3H^2} \rho_r, \quad \Omega_\Lambda \equiv \frac{\Lambda}{3H^2}, \quad \Omega_{\text{dr}} \equiv \frac{C}{S^4 H^2}, \quad \Omega_{k_{\text{eff}}} \equiv \frac{(k - \alpha)}{S^2 H^2}, \quad (7)$$

equation (3) reduces to,

$$H^2(z) = H_0^2 \left[\Omega_{m0} (1+z)^3 \left\{ 1 + \frac{\rho_{m0}}{2\sigma} (1+z)^3 + \frac{\rho_{r0}}{\sigma} (1+z)^4 \right\} + \Omega_{r0} (1+z)^4 \left\{ 1 + \frac{\rho_{r0}}{2\sigma} (1+z)^4 \right\} + \Omega_{\Lambda 0} + \Omega_{\text{dr}0} (1+z)^4 - \Omega_{k_{\text{eff}0}} (1+z)^2 \right]. \quad (8)$$

Constraints have been put on the brane tension σ by requiring that the relative corrections to the Newtonian gravity at short distances should be small. This constrains σ by $\sigma > 10^9 \text{ GeV}^4$ [17] giving $(\rho_{r0}/\sigma) < 10^{-61}$ and $(\rho_{m0}/\sigma) < 10^{-56}$. Thus the terms containing σ in equation (8) are significant only for the redshifts $z > 10^{15}$ and equation (8) reduces to the following in the later epochs:

$$H^2(z) = H_0^2 \left[\Omega_{m0} (1+z)^3 + (\Omega_{r0} + \Omega_{dr0})(1+z)^4 + \Omega_{\Lambda0} - \Omega_{k_{\text{eff}0}} (1+z)^2 \right]. \quad (9)$$

The *dark radiation* term is constrained by the big bang nucleosynthesis (BBN) by requiring that the change in the expansion rate due to this term be sufficiently small, so that an acceptable helium-4 abundance is produced. This yields $0 \leq \Omega_{dr0} \leq 0.11 \times \Omega_{r0}$ [18]. Note that the horizon condition of the black hole in the bulk requires that Ω_{dr} should be non-negative for the cases $k = 0$ and 1 [10, 11, 19]. By using the energy momentum conservation, the deceleration parameter $q \equiv -\ddot{S}/SH^2$ can be obtained from equation (3) in the form

$$q(t) = \frac{4\pi G}{3H^2}(\rho + 3p) - \frac{\Lambda}{3H^2} + \frac{C}{S^4 H^2} = \frac{\Omega_m}{2} + \Omega_r + \Omega_{dr} - \Omega_\Lambda. \quad (10)$$

The effective curvature index $(k - \alpha)$ in equations (3) and (9) now serves the role of the *dynamical curvature*, since the dynamics of the model, by using (9) at $z = 0$, can be written solely in terms of the source terms:

$$H^2 = H_0^2 [\{1 + z\Omega_{m0} + z(2+z)(\Omega_{r0} + \Omega_{dr0})\}(1+z)^2 - z(2+z)\Omega_{\Lambda0}]; \quad (11)$$

and it does not have any term of α . The same is true for other quantities, like the deceleration parameter and the expansion age of the universe, which do not have any term of α . However, the different distance measures do depend on α (at least for the non-zero k , as will become clear in the following), through the *dynamical curvature*. It should be noted that, unlike the standard cosmology, the *dynamical curvature* of the model is different from its *geometrical curvature* k , which has profound consequences in the model. To illustrate this point, we derive different distance measures in the model.

If a light source of redshift z is located at a radial coordinate distance r_1 , its *luminosity distance* d_L , *angular diameter distance* d_A and *proper motion distance* d_M are given by

$$d_L = (1+z)S_0 r_1, \quad d_A = \frac{S_0 r_1}{(1+z)}, \quad d_M = S_0 r_1, \quad (12)$$

where r_1 can be calculated from the metric (1), giving

$$\frac{1}{S_0} \int_0^z \frac{dz'}{H(z')} = \begin{cases} \sin^{-1} r_1, & \text{when } k = 1 \\ r_1, & \text{when } k = 0 \\ \sinh^{-1} r_1, & \text{when } k = -1. \end{cases} \quad (13)$$

It is worth noting that in deriving equations (12, 13), the only assumption one needs to make, is that of the validity of the RW metric given by equation (1) and hence they hold for all the RW models. The present *radius* of the universe S_0 , appearing in equations (12) and (13) which measures the curvature of spacetime, can be calculated from equation (7) as

$$S_0 = \sqrt{\frac{(k - \alpha)}{(\Omega_{\text{total}} - 1)}} H_0^{-1}, \quad \Omega_{\text{total}} \equiv \Omega_{m0} + \Omega_{r0} + \Omega_{dr0} + \Omega_{\Lambda0}. \quad (14)$$

An interesting case arises when the model is *geometrically flat* ($k = 0$). More explicitly, this case can be represented by $\Omega_{m0} + \Omega_{r0} + \Omega_{dr0} + \Omega_{\Lambda0} + \Omega_{\alpha0} = 1$, where the virtual Ω_α is defined by $\Omega_\alpha \equiv \alpha/S^2 H^2$. This is analogous to the case $\Omega_{m0} + \Omega_{r0} + \Omega_{\Lambda0} = 1$ of the standard flat cosmology. As the dynamics as well as the distances do not depend on α in the $k = 0$ model, Ω_{m0} , $\Omega_{\Lambda0}$, etc. can vary freely (by choosing suitable $\Omega_{\alpha0}$) and can produce an Ω_{total} significantly different from 1 (unlike the standard cosmology: $\Omega_{\text{total}} = 1$). This is, in fact, the only apparent difference (apart from Ω_{dr}) between the present ($k = 0$) model and the standard flat cosmology. In the latter case, the source parameters

are constrained to remain on the plane $\Omega_{m0} + \Omega_{r0} + \Omega_{\Lambda0} = 1$; whereas in the former case, they are free to be on the *family of planes* $\Omega_{m0} + \Omega_{r0} + \Omega_{dr0} + \Omega_{\Lambda0} + \Omega_{\alpha0} = 1$, parametrized by $\Omega_{\alpha0}$. The only other constraint the parameters have to satisfy is $1 + \Omega_{m0}z + z(2+z)\{\Omega_{r0} + \Omega_{dr0} - \Omega_{\Lambda0}/(1+z)^2\} \geq 0$, coming from equation (11). This gives more leverage to the parameters Ω_{m0} and $\Omega_{\Lambda0}$ and hence a bigger parameter space is allowed than in the flat standard cosmology. Additionally for a given α , one can still estimate S_0 (for the cases $\Omega_{\text{total}} \neq 1$) in a *geometrically flat* model through $S_0 = \sqrt{\alpha/(1 - \Omega_{\text{total}})}H_0^{-1}$, which is otherwise not possible in the standard cosmology. This implies that α is, respectively, positive or negative according as $\Omega_{\text{total}} < 1$ or $\Omega_{\text{total}} > 1$. For $\Omega_{\text{total}} = 1$, the model reduces to the standard flat model. In this paper, we shall keep ourselves limited to the case $k = 0$. A more general analysis will be done elsewhere [20].

We would like to mention about the alternative interpretations of the term α/S^2 appearing in equation (3). In fact, the $1/S^2$ fall off is a typical characteristic of a ‘pseudo’ source with equation of state $\rho + \sum_i p_i = 0$ which corresponds to topological defects, like cosmic strings and textures [21]. However, it neither contributes to the deceleration parameter nor to the Hubble parameter, as we have seen earlier. It would, therefore, be more appropriate to consider this term as a shift in the *dynamical curvature* of the standard cosmology and not as a source term.

III. OBSERVATIONS OF THE FLUCTUATIONS IN THE POWER SPECTRUM OF CMB

The small fluctuations (anisotropies) in the temperature of CMB offer a glimpse of the epoch in the early universe when photons decoupled from the cosmic plasma at $z_{\text{dec}} \approx 1100$. Before this epoch, matter and radiation were tightly coupled and behaved like a single fluid. At $z \approx 1100$, the temperature dropped sufficiently to let the protons capture electrons to form neutral hydrogen and other light elements (*recombination*). As the electrons, which had trapped photons, disappeared reducing the opacity for Thomson scattering, the photons *decoupled (last scattered)* from matter. The primordial quantum fluctuations, in matter as well as radiation, themselves may have their origin in the period of inflation. In the case of matter these fluctuations grew due to gravitational instability forming the present structure. However, the radiation has been streaming freely since decoupling. It has been highly redshifted, down to the micro region, and carry the picture of the last scattering surface left imprinted in the form of angular anisotropy in its intensity.

The initial fluctuations in the tightly coupled baryon-photon plasma oscillate at the speed of sound driven by gravity, inertia of baryons and pressure from photons. This continues until the recombination epoch. Physically these oscillations represent the hot and cold spots on the fluid generated by compression and rarefaction by a standing sound or acoustic wave. Thus the wave which has a density maximum at the time of last scattering, corresponds to a peak in the power spectrum. In the Legendre multipole space ℓ , this corresponds to the angle subtended by the sound horizon at the last scattering. Higher harmonics of the principal oscillations, which have oscillated more than once, correspond to secondary peaks. These locations of the peaks are very sensitive to the variations in the parameters of the model and hence serve as a sensitive probe to constrain the cosmological parameters and discriminate among various models [22, 23].

The angular power spectra of the temperature fluctuations in CMB have recently been measured in many experiments, like, BOOMERANG, MAXIMA, DASI, CBI, etc. [2, 3]. Bernardis et al have recently measured the ranges of the first three peaks from their improved analysis of a bigger sample of the BOOMERANG data [2]: $\ell_{\text{peak}_1} : 200 - 223$, $\ell_{\text{peak}_2} : 509 - 561$, $\ell_{\text{peak}_3} : 820 - 857$ at one sigma level; and $\ell_{\text{peak}_1} : 183 - 223$, $\ell_{\text{peak}_2} : 445 - 578$, $\ell_{\text{peak}_3} : 750 - 879$ at two sigma level. Though the uncertainties in these ℓ_{peak} values are large, all the observations made so far agree at least on the location of the first peak which has been measured comparatively more accurately.

The locations of the peaks are set by the acoustic scale ℓ_A , which can be interpreted as the angle subtended by the sound horizon at the last scattering surface. This angle (say, θ_A) is given by the ratio of sound horizon to the distance (*angular diameter distance*) of the last scattering surface:

$$\theta_A = \frac{S(t_{\text{dec}}) \int_0^{t_{\text{dec}}} c_s \frac{dt}{S(t)},}{d_A(t_{\text{dec}})}, \quad (15)$$

where the speed of sound c_s in the plasma is given by $c_s = 1/\sqrt{3(1+R)}$ and $R \equiv 3\rho_b/4\rho_\gamma = 3\Omega_{b0}/[4\Omega_{\gamma0}(1+z)]$ corresponds to the ratio of baryon to photon density. Acoustic scale $\ell_A = \pi/\theta_A$, in the $k = 0$ model, then yields

$$\ell_A = \pi \frac{\int_0^{z_{\text{dec}}} [\{1 + z\Omega_{m0} + z(2+z)(\Omega_{r0} + \Omega_{dr0})\}(1+z)^2 - z(2+z)\Omega_{\Lambda0}]^{-1/2} dz}{\int_{z_{\text{dec}}}^\infty c_s [\{1 + z\Omega_{m0} + z(2+z)(\Omega_{r0} + \Omega_{dr0})\}(1+z)^2 - z(2+z)\Omega_{\Lambda0}]^{-1/2} dz}. \quad (16)$$

The location of i -th peak in the angular power spectrum is given by

$$\ell_{\text{peak}_i} = \ell_A(i - \phi_i), \quad (17)$$

where the phase shift ϕ_i , caused by the plasma driving effect, is solely determined by the pre-recombination physics and hence would not have any significant contribution from the term containing α at that epoch. Thus one can safely approximate ϕ_i with its value in the standard cosmology [22], viz.

$$\phi_i \approx 0.267 \left\{ \frac{r(z_{\text{dec}})}{0.3} \right\}^{0.1}, \quad (18)$$

where $r(z_{\text{dec}}) \equiv \rho_r(z_{\text{dec}})/\rho_m(z_{\text{dec}}) = \Omega_{r0}(1 + z_{\text{dec}})/\Omega_{m0}$ is the ratio of radiation and matter energy densities at the decoupling era.

Note that Ω_{r0} gets contributions from photons (CMB) as well as neutrinos: $\Omega_r = \Omega_\gamma + \Omega_\nu$. The present photon contribution to the radiation can be estimated by the CMB temperature $T_0 = 2.728\text{K}$. This gives $\Omega_{\gamma 0} \approx 2.48 h^{-2} \times 10^{-5}$, where h is the present value of the Hubble parameter in units of $100 \text{ km s}^{-1} \text{ Mpc}^{-1}$. The neutrino contribution follows from the assumption of 3 neutrino species, a standard thermal history and a negligible mass compared to its temperature [24]. This supplies $\Omega_{\nu 0} \approx 1.7 h^{-2} \times 10^{-5}$. We have already mentioned that the allowed range of the *dark radiation* coming from the BBN is $[0 - 0.11] \times \Omega_{r0}$. We consider an average value from this range, viz., $\Omega_{\text{dr}0} = 5.5\%$ of Ω_{r0} . We find that the $\Lambda = 0$ model fits the observed peaks very well for a wide range of Ω_{b0} , Ω_{m0} and h . Figure 1 shows the ranges of Ω_{m0} and Ω_{b0} which produce the location of the first peak ℓ_{peak_1} in the observed region. In order to check the robustness of the model, we vary $\Omega_{\text{dr}0}$ at its extreme limits, i.e., 0% and 11% of Ω_{r0} . The resulting models also fit the observed peak locations very well. For example, for the values $\Omega_{m0} = 0.3$, $\Omega_{b0} = 0.05$ and $h = 0.65$, the different choices of $\Omega_{\text{dr}0}$ yield the following. (i) $\Omega_{\text{dr}0} = 0$: $\ell_{\text{peak}_1} = 197$, $\ell_{\text{peak}_2} = 467$, $\ell_{\text{peak}_3} = 737$; (ii) $\Omega_{\text{dr}0} = 0.055 \times \Omega_{r0}$: $\ell_{\text{peak}_1} = 199$, $\ell_{\text{peak}_2} = 473$, $\ell_{\text{peak}_3} = 748$; (iii) $\Omega_{\text{dr}0} = 0.11 \times \Omega_{r0}$: $\ell_{\text{peak}_1} = 201$, $\ell_{\text{peak}_2} = 479$, $\ell_{\text{peak}_3} = 756$.

It is obvious from the above that the influence of *dark radiation* on the locations of the peaks is to shift them towards higher ℓ values. This result is also consistent with other investigations [18]. One also notices that some of the above-mentioned ℓ_{peak} values are towards the lower boundary of the observations, especially when compared with 1-sigma observations. However, they can be increased either by decreasing h or by increasing Ω_{b0} . For example, even with $\Omega_{\text{dr}0} = 0$, the values $\Omega_{m0} = 0.3$, $\Omega_{b0} = 0.08$ and $h = 0.6$ yield $\ell_{\text{peak}_1} = 210$, $\ell_{\text{peak}_2} = 502$, $\ell_{\text{peak}_3} = 793$.

Just for comparison, it may be noted that the open model $\Lambda = 0$, $\Omega_{m0} = 0.3$, $\Omega_{b0} = 0.05$ with $h = 0.65$ in the standard cosmology ($\alpha = 0 = \Omega_{\text{dr}0}$) yields $\ell_{\text{peak}_1} = 425$, $\ell_{\text{peak}_2} = 1010$, $\ell_{\text{peak}_3} = 1594$, which is clearly ruled out by the observations. The favoured standard model: $\Omega_{m0} = 1 - \Omega_{\Lambda 0} = 0.35$, for $\Omega_{b0} = 0.05$ and $h = 0.65$, gives $\ell_{\text{peak}_1} = 222$, $\ell_{\text{peak}_2} = 524$, $\ell_{\text{peak}_3} = 827$.

IV. SUPERNOVAE IA OBSERVATIONS

SuperNovae (SN) Ia, which are thought to be thermonuclear explosions of carbon-oxygen white dwarfs [25], are almost universally regarded as *standard candles* and can be observed at cosmological scales since they have high enough absolute luminosity. As the *luminosity distance* d_L depends sensitively on the spatial curvature and the expansion dynamics of the models, the magnitude-redshift (m - z) relation for the high redshift SN Ia can be used as a potential test for cosmological models and provides a useful tool to constrain the parameters of the models.

In order to fit to our model, we consider the data on the redshift and magnitude of a sample of 54 SN Ia considered by Perlmutter et al (excluding 6 outliers from the full sample of 60 SN) [26], together with SN 1997ff at $z = 1.755$, the highest redshift supernova observed so far [27]. It has been confirmed now that SN 1997ff has been observed on the brighter side due to gravitational lensing from the galaxies lying on the line of sight [28]. After correction for lensing, the revised magnitude of this SN is $m^{\text{eff}} = 26.02 \pm 0.34$ [28] which we shall use in our calculations.

The standard definition of magnitude $m(z)$ for the RW spacetime (1) is given by [29]

$$m(z) = \mathcal{M} + 5 \log[\mathcal{D}_L(z)], \quad (19)$$

where $\mathcal{M} \equiv (M - 5 \log H_0 + \text{constant})$ is the *Hubble constant-free* absolute luminosity, M is the absolute luminosity of the source and $\mathcal{D}_L \equiv H_0 d_L$ is the dimensionless luminosity distance. The luminosity distance d_L in the model is supplied by equations (11–13). It has been shown in [16] that the *dark radiation* term can be safely neglected while

considering the present SN Ia data. Moreover, the radiation terms can be neglected even at $z = 3.8$ (which corresponds to the highest redshift quasar we shall be considering in the next section) since the contribution of the term $\Omega_{r0} + \Omega_{dr0}$ at $z = 3.8$ (even when Ω_{dr0} is at its highest limit) in equation (9) is only about 0.2% of the contribution from the term Ω_{m0} with $\Omega_{m0} = 0.3$. The χ^2 value is calculated from its usual definition

$$\chi^2 = \sum_{i=1}^{55} \left[\frac{m_i^{\text{eff}} - m(z_i)}{\delta m_i^{\text{eff}}} \right]^2, \quad (20)$$

where m_i^{eff} refers to the effective magnitude of the i th SN which has been corrected by the lightcurve width-luminosity correction, galactic extinction and the K-correction from the differences of the R- and B-band filters and the dispersion δm_i^{eff} is the uncertainty in m_i^{eff} .

There seems to be a general impression that the high redshift SN observations rule out the decelerating models. However, this is not true even in the standard cosmology, as we shall see in the following. Equation (10) suggests that the present universe will be accelerating if $\Omega_{\Lambda 0} > \Omega_{m0}/2$. Thus the best-fitting standard model to this sample, which is obtained for the values $\Omega_{m0} = 0.7$, $\Omega_{\Lambda 0} = 1.2$, is of course accelerating. The $\Delta\chi^2$ (χ^2 per degrees of freedom), for this fitting, is obtained as 1.09 and the probability Q , which measures the goodness of fit [30], is obtained as 29.7% which represent an excellent fit. Even the best-fitting flat model in the standard cosmology is an accelerating one, which is obtained as $\Omega_{m0} = 1 - \Omega_{\Lambda 0} = 0.3$ with $\Delta\chi^2 = 1.11$ and $Q = 26.6\%$. Though the canonical Einstein-deSitter model ($\Omega_{m0} = 1 - \Omega_{\Lambda 0} = 1$) has a poor fit: $\Delta\chi^2 = 1.72$ and $Q = 0.08\%$ and is ruled out, however, the open models with low Ω_{m0} have reasonable fits. For example, the decelerating (standard cosmological) models $\Omega_{m0} = 0.2$ with $\Lambda = 0$ ($\Delta\chi^2 = 1.24$, $Q = 11.4\%$); $\Omega_{m0} = 0.3$ with $\Lambda = 0$ ($\Delta\chi^2 = 1.27$, $Q = 8.5\%$); $\Omega_{m0} = 0.4$ with $\Lambda = 0$ ($\Delta\chi^2 = 1.32$, $Q = 5.7\%$), etc., have reasonable fittings and by no means are rejectable. Open decelerating models with non-zero Λ ($0 < \Omega_{\Lambda 0} < \Omega_{m0}/2$) have even better fit.

In the present (geometrically flat) brane model with $\Lambda = 0$, χ^2 decreases for lower values of Ω_{m0} (as in the standard open cosmology) giving the best-fitting solution for $\Omega_{m0} = -0.3$ (with $\Delta\chi^2 = 1.19$, $Q = 16.5\%$), which is though unphysical. Thus a ‘physically viable’ best-fitting solution can be regarded as $\Omega_{m0} = 0$, which gives $\Delta\chi^2 = 1.22$ with $Q = 12.4\%$, representing a reasonably good fit, though not as good as the best fit in the standard cosmology. The allowed regions by the data in the $\Omega_{m0} - \mathcal{M}$ plane are plotted in Figure 2 at 1, 2 and 3 sigma levels.

V. ANGULAR SIZE-REDSHIFT DATA FOR HIGH REDSHIFT COMPACT RADIO SOURCES

The radio sources are attractive for the test of cosmological models because they are usually identified with quasars which, in general, have high redshifts, so the models may be more easily distinguished than with the extended double-lobed sources. Kellermann [31] showed, by using a sample of 79 such sources, that the resulting angular size-redshift (Θ - z) relation was cosmologically credible. Jackson and Dodgson [32] used his data to test the standard cosmology with a cosmological constant. Later on, a more extensive exercise was carried out by Jackson and Dodgson [33] by considering a bigger sample of 256 ultracompact sources selected from the compilation from Gurvits [34]. It is, in fact, this data set we are considering to test the present model. Although this data set has been extended recently by Gurvits et al [35], however, the modified sample becomes highly inhomogeneous as it compiles many different data sets obtained by many different observers using different instrumentations and imaging techniques. Hence its credibility is lost and it can fit any model [6].

The original data set of Jackson and Dodgson [33] (which we are considering here) was selected from a bigger sample of 337 sources, out of which Jackson and Dodgson selected the sources with z in the range 0.5 to 3.8. These objects, 256 in number, are ultra compact radio sources having angular sizes of the order of a few milliarcseconds. They are deeply embedded in the galactic nuclei and have very short life time compared with the age of the universe. Thus they are expected to be free from the evolutionary effects and hence may be treated as *standard rods*, at least in the statistical sense. These sources are distributed into 16 redshift bins, each bin containing 16 sources. This compilation has recently been used by many authors to test different cosmological models [7, 36].

In order to fit the data to the model, we derive the Θ - z relation in the following. The (apparent) angular size Θ of a source, whose proper diameter is d , is given by

$$\Theta(z) = \frac{0.0688 d h}{\mathcal{D}_A(z)} \text{ milliarcseconds}, \quad (21)$$

where $\mathcal{D}_A \equiv H_0 d_A$ is the dimensionless angular diameter distance and d is measured in pc. In the present model, d_A can be obtained from equations (11–13). We fix $\Lambda = 0$ and calculate the theoretical $\Theta(z)$ for a wide range of parameters Ω_{m0} and dh . χ^2 is computed from

$$\chi^2 = \sum_{i=1}^{16} \left[\frac{\Theta_i - \Theta(z_i)}{\delta\Theta_i} \right]^2, \quad (22)$$

which measures the agreement between the theoretical $\Theta(z_i)$ and the observed value Θ_i with the errors $\delta\Theta_i$ of the i th bin in the sample.

Here also χ^2 decreases for lower values of Ω_{m0} giving the best-fitting solution for $\Omega_{m0} = -0.15$ with $\Delta\chi^2 = 0.94$, $Q = 51.9\%$, which is though not interesting. The ‘viable’ best-fitting solution for $\Omega_{m0} = 0$ yields $\Delta\chi^2 = 0.95$ with $Q = 50.4\%$, which represents an excellent fit. Figures 3 shows the allowed regions by the data in the parameter space $\Omega_{m0} - dh$ at 1, 2 and 3 sigma levels.

VI. CONCLUSION

The best-fitting models to the high redshift supernovae Ia observations predict an accelerating expansion of the universe driven by some unknown smooth fluid with negative pressure, like the cosmological constant Λ . Although the open low energy standard models without this strange fluid show reasonable fit to the SN Ia data, they are ruled out by the recent CMB observations which predict that the universe is spatially flat. This has given rise to a plethora of models of the hypothetical ‘dark energy’ (variants of Λ) which do not seem to resemble any known form of matter tested in the laboratory.

In this paper, we have presented a warped brane model wherein the addition of the brane curvature scalar as a surface term in the action results in shifting the *geometrical curvature* index k of the standard cosmology by a constant α . Though α does not enter directly into the expressions for the Hubble parameter and the different distances measured in the geometrically flat ($k = 0$) model, however it helps Ω_{total} to assume values different from 1, which has profound consequences. Even for $\Lambda = 0$, the low energy model successfully explains the observed locations of the peaks in the angular power spectrum of CMB. The model also fits the high redshift supernovae Ia observations, taken together with the recently observed SN 1997ff at $z \approx 1.7$. Additionally, it also fits the data on the angular size and redshift of the compact radio sources very well.

Though α and S_0 do not enter into the dynamics of the (geometrically flat) model, we can still extract some constraint on the sign of α from the observations, which can be done through the relation $\alpha/S_0^2 H_0^2 = 1 - \Omega_{\text{total}}$. Obviously, the SN Ia and the radio sources data, which favour low density models (see Figures 2 and 3) predict a positive α . However, the CMB observations are consistent with either sign of α (see Figure 1) for the available accuracy of the data. This degeneracy might be removed by the future observations from the MAP and PLANCK experiment which are expected to give more accurate measurements.

It is interesting to note that the low Ω_{m0} models, which are consistent with all the three observations we have considered, are also consistent with the dynamical measurements of the energy density. Moreover, they are also consistent with the age of the oldest objects detected so far, e.g., the globular clusters of age $t_{GC} = 12.5 \pm 1.2$ Gyr [37]. In this connection, we notice that the recent measurements of H_0 favour a value in the range $(61 - 65) \text{ km s}^{-1} \text{ Mpc}^{-1}$ [38], setting the age of the universe t_0 in the following ranges. $\Omega_{m0} = 0.3$: $t_0 \in (12.2 - 13.0)$ Gyr; $\Omega_{m0} = 0.2$: $t_0 \in (12.7 - 13.6)$ Gyr, which are consistent with the above-mentioned t_{GC} . A large number of other methods appear to converging on a value of H_0 in the range $(60 - 80) \text{ km s}^{-1} \text{ Mpc}^{-1}$ [39]. An average value of $H_0 = 65 \text{ km s}^{-1} \text{ Mpc}^{-1}$ from this range constrains Ω_{m0} of the model by $\Omega_{m0} \leq 0.34$ to give $t_0 \geq 12$ Gyr.

Acknowledgements: We thank Naresh Dadhich, Wayne Hu, Roy Maartens, Jayant Narlikar, T Padmanabhan and Kandaswamy Subramanian for useful comments and discussions. Thanks are also due to Paolo de Bernardis for sending the observed ranges of the CMB peaks. RGV thanks DAE for his Homi Bhabha postdoctoral fellowship and PS thanks CSIR for his research fellowship.

-
- [1] Peebles P. J. E. and Ratra Bharat, *astr0-ph/0207347*;
Sahni V. and Starobinsky A. 2000 *Int. J. Mod. Phys. D* **9** 373.
 - [2] de Bernardis P. et al 2002 *Astrophys. J.* **564**, 559.
 - [3] de Bernardis P. et al 2000 *Nature* **404**, 955;
Lee A. T. et al 2001 *Astrophys. J.* **561**, L1;
Halverson N. W. et al 2002 *Astrophys. J.* **568**, 38;
Sievers J. L. et al, *astro-ph/0205387*.

- [4] Turner M. S., astro-ph/0106035.
- [5] Vishwakarma, R. G. 2002 Class. Quantum Grav. **19**, 4747;
Vishwakarma, R. G. 2002 MNRAS, **331**, 776;
Vishwakarma, R. G. 2001 Gen. Relativ. Grav. **33**, 1973.
- [6] Vishwakarma, R. G. 2001 Class. Quantum Grav. **18**, 1159.
- [7] Vishwakarma, R. G. 2000 Class. Quantum Grav. **17**, 3833.
- [8] Narlikar J. V. and Padmanabhan T. 2001 Ann. Rev. Astron. Astrophys. **39**, 211;
Boisseau B, Esposito-Farese G., Polarski D. and Starobinsky A. A. 2000 Phys. Rev. Lett. **85**, 2236;
Esposito-Farese G. and Polarski D. 2001 Phys. Rev. D **63**, 063504;
Gaztanaga E. and Lobo A. 2001 Ap. J. **548**, 47;
Narlikar J. V., Vishwakarma, R. G., Hajian Amir, Souradeep Tarun, Burbidge G. and Hoyle F. 2002 (to appear in Astrophys. J.), astro-ph/0211036
Bayin Selcuk S. 2002 (to appear in IJMPD), astro-ph/0211097.
- [9] Israel W. 1966 Nuov. Cim. B **44**, 1.
- [10] Mukohyama S., Shiromizu T. and Maeda K. 2000 Phys. Rev. D **62**, 024028.
- [11] Kraus P. 1999 JHEP **9912**, 011.
- [12] Binetruy P., Deffayet C., Ellwanger U. and Langlois D. 2000 Phys. Lett. B **477**, 285.
- [13] Balasubramanian V and Kraus P. 1999 Comm. Math. Phys. **208**, 413.
- [14] Kim N. J., Lee H. W. and Myung Y. S. 2001 Phys. Lett. B **504**, 323.
- [15] Collins H. and Holdom B. 2000 Phys. Rev. D **62**, 105009;
Shtanov Yu. V., hep-th/0005193.
- [16] Singh P., Vishwakarma R. G. and Dadhich N., hep-th/0206193.
- [17] Maartens R. et al 2000 Phys. Rev. D **62**, 041301.
- [18] Ichiki K. et al 2002 Phys. Rev. D **66**, 043521.
- [19] Singh P. and Dadhich N., hep-th/0204190;
Singh P. and Dadhich N., hep-th/0208080.
- [20] Vishwakarma R. G. and Singh P., *In preparation*.
- [21] Vilenkin A. and Shellard E. P. S. 1995 *Cosmic strings and other topological defects*, (Cambridge U. Press);
Dadhich N. and Narayan N. 1998 Gen. Relativ. Grav. **30**, 1133;
Dadhich N. and Patel L. K. 1999 Pramana **52**, 359;
Babul A. et al 1987 Astrophys. J. **316**, L49;
Gregory R. 1989 Phys. Rev. D. **29**, 2108;
Dabrowski M. P. 1989 Astron. J. **97**, 978.
- [22] Hu W., Fukugita M., Zaldarriaga M. and Tegmark M. 2001 Astrophys. J. **549**, 669.
- [23] Doran M. and Lilley M. 2002 MNRAS **330**, 965;
Doran M. and Lilley M., Schwindt J. and Wetterich C. 2001 Astrophys. J. **559**, 501.
- [24] Hu Wayne and Dodelson Scott 2002 Ann. Rev. Astron. Astrophys.
- [25] Trimble V. 1983 Rev. Mod. Phys. **54**, 1183
Woosley S. E. and Weaver T. A. 1986 ARA & A **24**, 205.
- [26] Perlmutter S., et al 1999 Astrophys. J. **517**, 565.
- [27] Riess A. G., et al 2001 Astrophys. J. **560**, 49.
- [28] Narciso B., et al, astro-ph/0207097.
- [29] Weinberg S. 1972 *Gravitation and Cosmology*, (New York, John Wiley).
- [30] Press W., Teukolsky S., Vetterling W. and Flannery B. 1992 *Numerical Recipes* chapter 15, (Cambridge University Press).
- [31] Kellermann K I 1993 Nat. **361** 134.
- [32] Jackson J C and Dodgson M 1996 MNRAS **278** 603.
- [33] Jackson J C and Dodgson M 1997 MNRAS **285** 806.
- [34] Gurvits L I 1994 Astrophys. J. **425** 442.
- [35] Gurvits L I, Kellermann K I and Frey S. 1999 Astron. Astrophys. **342** 378.
- [36] Banerjee S K and Narlikar J V 1999 MNRAS **307** 73.
- [37] Cayrel R., et al 2001 Nature, **409**, 691.
Gnedin O. Y., Lahav O. and Rees M. J., astro-ph/0108034.
- [38] Passnacht C. D. et al astro-ph/0208420.
- [39] Freedman W. B. 2000 Phys. Rept. **333**, 13.

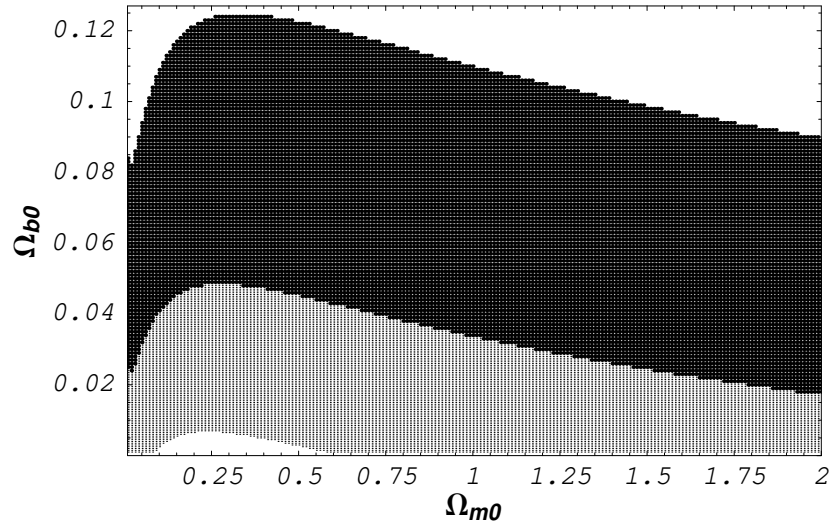


FIG. 1: The allowed regions by the CMB at 1 and 2 sigma levels are shown in the $\Omega_{m0} - \Omega_{b0}$ plane, which produce the first peak in the ranges, respectively, 200 – 223 (dark-shaded region) and 183 – 223 (light-shaded + dark-shaded regions). We have considered $\Omega_{dr0} = 0.055 \times \Omega_{r0}$ and $h = 0.65$.

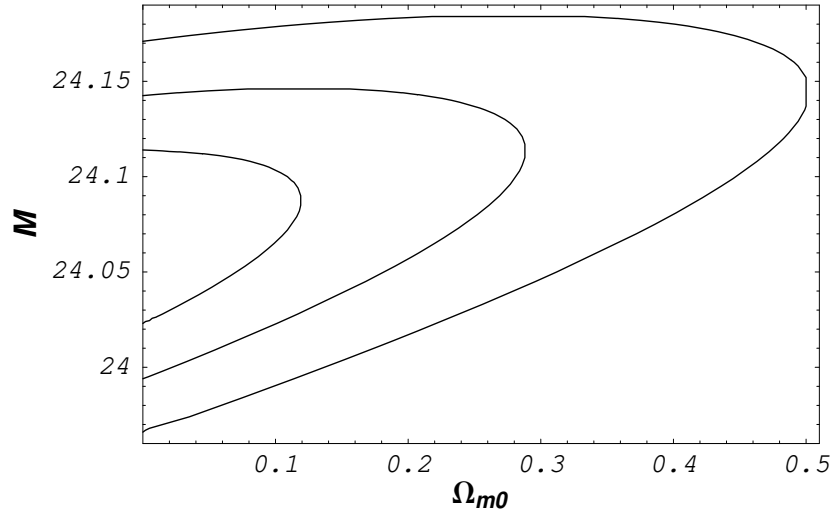


FIG. 2: The allowed regions by the SN Ia observations are shown in the $\Omega_{m0} - M$ plane ($M \equiv$ the *Hubble constant-free* absolute luminosity). The ellipses, in the order of increasing size, correspond to respectively 1, 2 and 3 sigma levels.

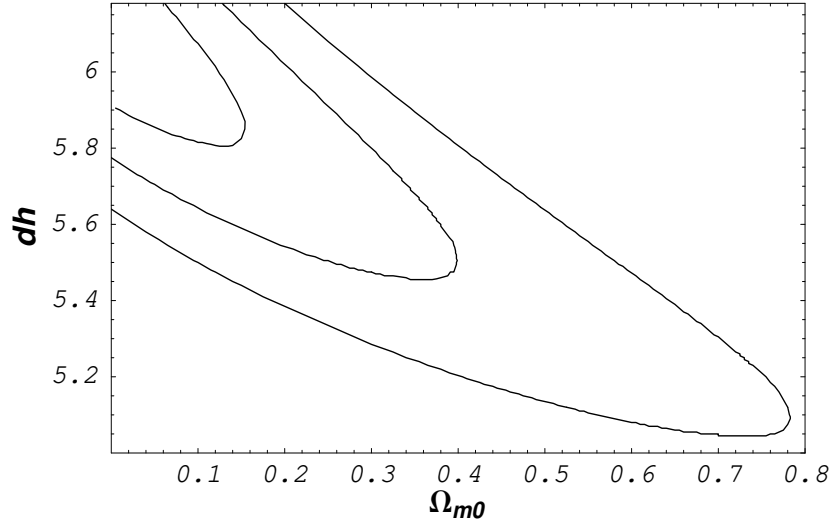


FIG. 3: The allowed regions by the compact radio sources data are shown in the $\Omega_{m0} - dh$ plane (where d is measured in pc). The ellipses, in the order of increasing size, correspond to respectively 1, 2 and 3 sigma levels.